Proceedings of ISFOG 2025
5TH INTERNATIONAL SYMPOSIUM ON
FRONTIERS IN OFFSHORE GEOTECHNICS
Nantes, France | June 9-13 2025

ISBN 978-2-85782-758-0

A finite element implementation for cohesive soils of PISA design model for offshore wind turbines foundations

Vincenzo Germano*
Cathie Group, London, UK

Christophe Jaeck
Cathie Group, Brussels, Belgium

* *Vincenzo.Germano@cathiegroup.com (corresponding author)*

ABSTRACT: In the offshore energy industry, the lateral soil-pile interaction has been traditionally modelled by means of springs calibrated by non-linear and depth dependent soil reaction curves known as p-y curves.
It became evident that this approach led to an underestimation of the lateral stiffness of monopiles of relatively low values of length-to-diameter ratio that are typically adopted for offshore wind turbine structures, resulting in an underestimation of the eigenfrequencies and generally oversizing of the foundation structures.
Updated methods are now commonly implemented in the industry. One of the methods was developed in the framework of the PISA project, based on onshore lateral pile tests in both sand and clay. The enhanced soil response curves based on PISA method need to be calibrated against the results of full 3D Finite Element simulations of the soil-pile interaction. In cohesive soils, this was undertaken by running numerical analyses using advanced soil models not commercially available, calibrated considering the pile tests results conducted in stiff clay till of the Cowden site.
Different approaches were proposed aiming to replicate the PISA JIP outcome by adopting commercially available soil models with reasonable results but never fully comparable to the in-situ pile tests results in cohesive soils.
In this paper, a calibration procedure is proposed for the commercially available Hardening Soil with Small Strain soil model. The model calibration is tested by simulating the pile tests conducted in Cowden till. Results of the lateral pile response show good matching with the full-scale pile test data.

Keywords: Monopile design; PISA method; soil-structure interaction; numerical analysis; constitutive model

1 INTRODUCTION

Offshore wind farms have become an important source of renewable energy. In the last decade, many offshore wind parks have been installed as part of the energy policy of major European countries and it is becoming the crucial investment policy for major countries such as China and USA.

For relatively shallow waters (generally less than 50m), one of the most common foundation concepts is the monopile, i.e., a larger diameter open-ended steel tube driven into the soil. The generated lateral loads and overturning moments generally govern the design of monopiles supporting a wind turbine.

Traditionally, in the offshore energy industry, the lateral soil-pile interaction is modelled by means of non-linear and depth dependent soil reaction curves known as p-y curves.

The relatively recently completed PISA (PIle Soil Analysis) project (Byrne et al., 2020) has proved that the traditional p-y curves are not appropriate for monopiles with low length-to-diameter (L/D) ratio used for offshore wind turbine foundations. It demonstrates that the traditional p-y method without modifications results in an underestimation of the lateral stiffness, hence also of the eigenfrequencies, and general oversizing of the foundation structure.

Based on these results, the PISA project provided a framework where the traditional method based on the sole reaction forces normal to the pile shaft is extended to include additional components such as moment and shear forces along the shaft and at the pile tip. The calibration of these new soil response curves is based on the performance of full 3D Finite Element analyses of the soil-pile interaction.

Use of a FE analysis requires the selection of the most appropriate soil constitutive model, depending on the soil behaviour aspects that are required for the simulation. The FE analyses undertaken for the PISA project were performed using advanced constitutive models for soils. In the specific case of a lateral loaded monopile in the Cowden clay till, the constitutive model adopted was developed in the framework of the critical state soil mechanics. This model represents an enhancement of the modified Cam Clay model (Roscoe and Burland, 1968), which accurately simulates aspects of the mechanical behaviour of low plasticity and overconsolidated clay such as the Cowden till. Key enhancements of the this model are: i) non-linear Hvorslev yield surface introduced on the "dry side" (overconsolidation ratio greater than 2) to better capture the behaviour of overconsolidated clays and overcome the excessive strength overestimation provided by the modified Cam Clay model, ii) adopting of Van Eekelen formulation for yield and plastic potential surfaces in the deviatoric plane, accounting for shear strength variation with Lode's angle (e.g., triaxial compression vs. extension) and, iii) incorporate stress- and strain-dependent stiffness, reflecting the non-linear pre-yield response. Details of the mathematical formulation of this model are provided by Zdravković et al. (2020a). Although this enhanced critical state-based model represent the ideal solution for the replication of clay behaviour, this is not easily available in the everyday engineering practice. Several attempts have been made to replicate the soil-monopile interaction in clay using constitutive models formulated in terms of total stress (Minga and Burd, 2019 and Kaltekis et al., 2023). Although these results have shown reasonable match with the real-scale pile testing outcomes, none of these simulations has been able to reach a similar level of correspondence with the real scale pile test data as obtained with the advanced soil models adopted in the PISA project.

In this paper, a calibration procedure for a known and everyday suitable constitutive model of soils formulated in terms of effective stresses is investigated and presented. Using the site-specific characterization data of the stiff clay till of the Cowden site as presented in Zdravković et al. (2020a), the Hardening Soil with Small strain stiffness (HSS) (Schanz et al., 1999), (Benz, 2007) model is calibrated and used for the 3D FE soil-monopile interaction analysis.

The HSS model is a combination of the Hardening Soil model proposed by Schanz et al. (1999) and the elastic small strain overlay model developed by Benz (2007). The Hardening Soil model is an isotropic hardening elasto-plastic model developed in terms of effective stresses, characterized by two yield surfaces: a shear hardening yield surface and a cap yield surface. This latter is introduced to delimit the elastic region for compressive stress paths. The shear hardening yield surface is a function of the deviatoric plastic strain with a non-associated flow rule and it can expand up to the Mohr-Coulomb failure criterion, whereas the cap yield surface is governed by plastic volumetric strain and an associated flow rule according to the modified Cam Clay model. The incorporated elastic small strain overlay model allows stiffness dependence from stress and strain for pre-yielding conditions. The shape of the model in the deviatoric plane will appear hexagonal (dry side with high OCR) or circular (wet side with low OCR). Details of the mathematical formulation of this model are provided by Schanz et al. (1999) and Benz (2007).

Designed primarily for granular soils, the HSS model has been proven widely applicable to cohesive soils, both under static (Surarak et al., 2012) and seismic conditions (Amorosi et al., 2016). While quite versatile and of easy calibration, the HSS formulation has limitations such as: 1) inability to replicate negative hardening (softening) typically occurring for high over consolidated soils under deviatoric stress conditions, 2) inability to account for strength anisotropy due to its isotropic hardening formulation and 3) inability to satisfactorily predict large excess pore water pressure build up and ratcheting under cyclic loading. However, as shown in this paper and confirmed in the existing literature, with an appropriate and careful calibration, these limitations can be minimised and good results obtained.

For the scope of the present work, the FE software packages used for this simulation is © Plaxis 3D Connect Edition V21.01 (Plaxis, 2021), one of the most popular geotechnical commercial software implementing the HSS model.

2 GROUND MODEL OF COWDEN SITE

Cowden, located in the north-east England, is one of the two sites selected for the PISA pile testing campaign. This site provides a ground profile characterised by over-consolidated low-plasticity glacial clay till which is representative of various North Sea windfarm sites. An extensive interpretation of the historic and most recent test data on Cowden till are presented by Ushev (2017). The reference soil profiles adopted at the Cowden site were defined following the interpretation provided by Zdravković et al. (2020a). The main soil properties profiles are shown in Figure 1 and Figure 2. In the same figures, these profiles are compared to the profiles adopted for the FE ground model initialization presented in this study (reference profiles). The undrained strength profile shown in Figure 2 is representative of Cowden till behaviour under triaxial compression.
A total unit weight of 21.19 kN/m^3 was adopted as indicated by Zdravković et al. (2020a).

3 CALIBRATION OF HSS MODEL

In the present section the initialization, as well as the strength and stiffness calibration of the HSS model are presented. The full set of HSS parameters calibrated for the 3D FE analyses are given in Appendix. To best replicate the in-situ initial conditions of the stress history parameters (K_0 and *OCR*), undrained shear strength and stiffness, the ground profile was subdivided in twelve sub-layers.

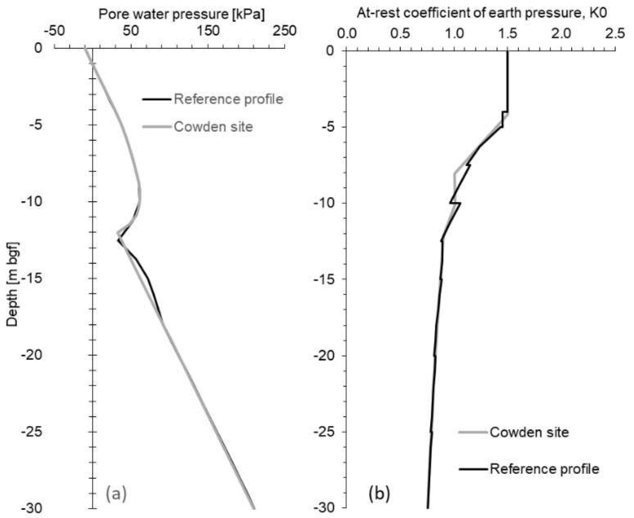

Figure 1 - Profiles of initial state parameters (1/2)

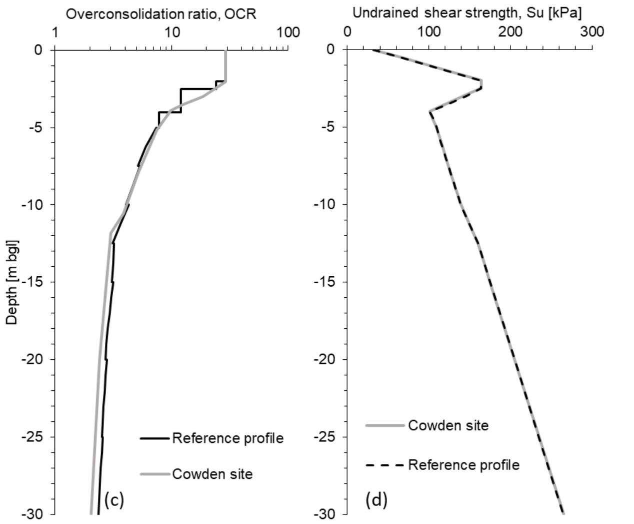

Figure 2 - Profiles of initial state parameters (2/2)

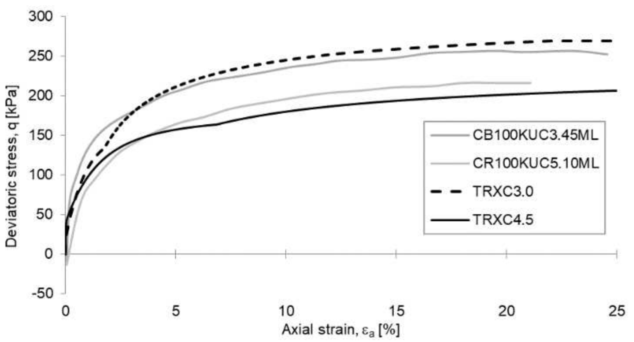

Figure 3 - Stress-strain response of HSS model (TRXC)

3.1 Model initialization

The initialization of HSS model has been achieved by defining the initial vertical and horizontal stress distribution with depth according to the K_0-procedure (Plaxis, 2021) and the definition of the OCR profile with depth which sets-up the initial size of the cap yield surface.

3.2 Calibration of strength parameters

The effective strength parameters required for the calibration of the HSS model are the effective cohesion (c') and the angle of shear resistance (ϕ'). These parameters have been derived by finding the equivalence of the undrained strength profile provided by the HSS model to the design profile shown in Figure 2d. For this scope, a two-step approach was adopted, consisting of:

1. Definition of an angle of shear resistance back calculated from the analytical solution of the undrained shear strength response formulated in terms of critical state soil mechanics (Potts and Zdravković, 1999):

$$S_u = g(\theta)cos(\theta)\sigma'_v \frac{OCR}{6}(1 + 2K_0^{NC})(1 + B^2)\left[\frac{2(1+2K_0^{OC})}{OCR(1+2K_0^{NC})(1+B^2)}\right]^{\frac{\kappa}{\lambda}} \quad (1)$$

   with $B = \frac{\sqrt{3}(1-K_0^{NC})}{g(\theta)(1+2K_0^{NC})}$ where $g(\theta) = sin(\phi')/[cos(\theta) + sin(\theta)sin(\phi')/\sqrt{3}]$ is the slope of the critical state line based on the Mohr-Coulomb hexagonal yield shape which simulate triaxial compression and extensions with Lode's angle $\theta = -30°$ and $\theta = 30°$, respectively. Given the inability of the HSS model to account for different strengths in compression and extension, the aim of this first step is to define a unified value of the angle of shear resistance representative of both compression and extension. The dilatancy angle is always kept equal to zero.
2. Definition and optimization of the effective cohesion values by simulating isotopically consolidated undrained triaxial tests in compression with the HSS model. Selected stress-strain curves are compared in Figure 3 where, for similar ranges of depths, the results of the simulation (black lines) are compared to the laboratory test data (grey lines). In this figure, the depth of the test expressed in metres is represented by the numbers next to the test name. For the

simulated tests, the depth refers to the middle point of the discretised sub-layer.

The undrained shear strength values obtained by replicating the isotopically consolidated undrained triaxial test results up to depths of the PISA test piles are plotted in Figure 4 where they are compared to the reference undrained profile and the undrained strength profiles for triaxial compression and extension obtained with Equation 1.

3.3 Calibration of stiffness parameters

The calibration of the HSS model requires two sets of stiffness parameters (Benz, 2007). The first set of parameters comprises the reference stiffness modulus at 50% of failure (E_{50}^{ref}), the reference oedometric stiffness modulus (E_{oed}^{ref}) and the reference unloading-reloading stiffness modulus (E_{ur}^{ref}), used for the definition of the stiffness stress-dependency. The second set consists of the two parameters used to define the stiffness strain-dependency: the reference elastic small strain shear modulus (G_0^{ref}) and a reference threshold shear strain ($\gamma_{0.7}^{ref}$). The dependency on the stress level of the four reference stiffness moduli is then controlled by a parameter m ranging from 0 (no dependency) to 1 (linear dependency).

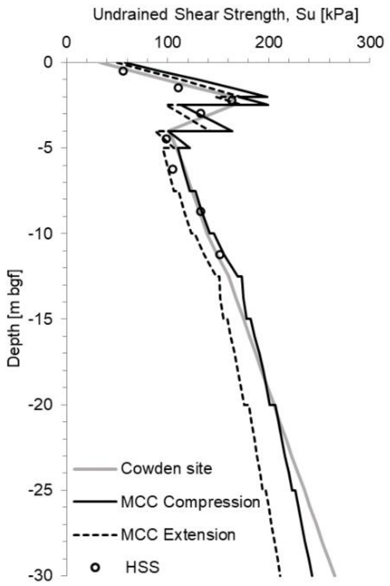

Figure 4 - Simulated undrained strength

1. Based on the profile of the small strain shear stiffness (Figure 5), a reference value G_0^{ref} is initially defined as the small strain shear stiffness value corresponding to a reference mean effective stress p'_{ref} equal to 100kPa.
2. From G_0^{ref}, the reference value of the shear stiffness corresponding to 50% of the maximum deviatoric stress at failure is calculated according to Equation 2 where the degradation of the stiffness ratio is controlled by the parameter $0 < g < 1$ (Mayne et al., 2009). In this case an average value of 0.03 is selected to best represent the laboratory test results.

$$\frac{G_{50}^{ref}}{G_0^{ref}} = \left[1 - \left(\frac{q}{q_f}\right)^g\right] \tag{2}$$

The reference stiffness modulus at 50% of failure is calculated following the standard relationship of the elastic theory, i.e., $E_{50}^{ref} = 2(1+\nu)G_{50}^{ref}$, using a Poisson's ratio for the Cowden till of 0.28 (Ushev, 2017).

3. The reference oedometric and unloading-reloading stiffnesses are then calculated: $E_{oed}^{ref} = 0.8E_{50}^{ref}$ and $E_{oed}^{ref} = 3E_{50}^{ref}$ (Schanz et al., 1999).
4. The threshold shear strain $\gamma_{0.7}$ is calculated according to the relationship proposed by Darendeli and Stokoe (2001), function of the mean effective pressure p', the reference threshold shear strain and a factor N assumed equal to 0.35 according to the authors (Equation 3).

$$\gamma_{0.7} = \gamma_{0.7}^{ref}\left(\frac{p\prime}{p'_{ref}}\right)^N \tag{3}$$

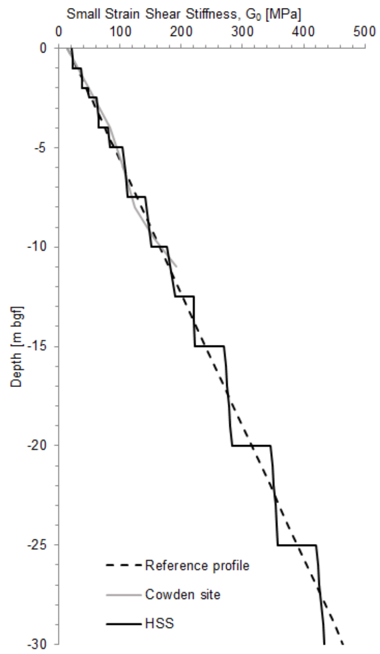

Figure 5 - Initial small strain shear stiffness profile

The small strain shear stiffness profile provided by the HSS model for the initialization of the finite element analysis is shown in Figure 5. Figure 6 compares the model response curves in terms of stiffness degradation with strain level to the measured ranges of decay curves from different projects (grey lines) at the Cowden site (Zdravković et al., 2020a).

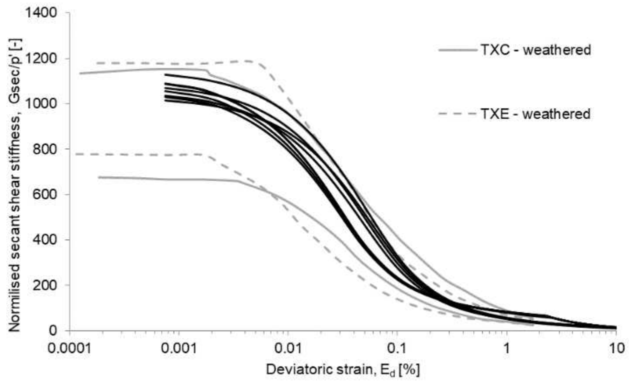

Figure 6 - Measured stiffness ranges compared to simulated stress normalised shear stiffness reduction

4 FE SIMULATION OF THE LATERAL LOADED MONOPILE

The analyses were undertaken with the Finite Element (FE) commercial package Plaxis 3D (Plaxis, 2021).

To account for the plane of symmetry of a laterally loaded pile, only half of the domain was discretised where the origin of the global system of reference (i.e., X=Y=Z=0) is at the ground level along the pile vertical axis of symmetry (Figure 7).

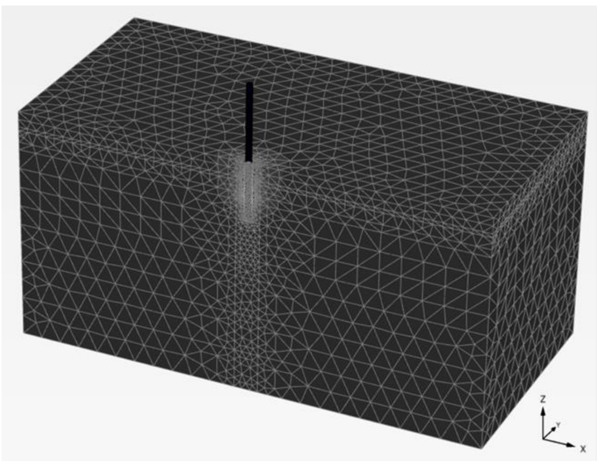

Figure 7 - Example of adopted 3D mesh

Piles of four distinct geometries were installed at Cowden site for testing (Zdravković et al., 2020b). A summary of the pile geometries is summarised in Table 1. For the purposes of the present study two cases where considered, i.e., the CM3 and CL2 pile geometries. All piles included a 10m stickup height.

The vertical boundaries were located at 30m and 80m from the pile central axis for the CM3 and CL2 pile geometries, respectively. The bottom boundary was located at 30m and 40m below the ground level for the CM3 and CL2 test piles, respectively, hence at 22.4m (29.4 pile diameters) and 29.5m (14.75 pile diameters) underneath the pile tip elevation.

Table 1. Geometric properties of tested pile.

Pile	Diameter, D	Embedded length, L	L/D	Pile wall thickness, t
	[m]	[m]	[-]	[mm]
CM2	0.762	2.3	3.00	10
CM9	0.762	4.0	5.25	13
CM3	0.762	7.6	10.0	25
CL2	2.0	10.5	5.25	25

The steel material adopted for the pile was assumed to be linear elastic, with a Young's modulus of 200GPa and a Poisson's ratio of 0.30. The pile was modelled weightless and assumed to be wished in place, thus ignoring any installation effect.

The outer soil-pile interface was discretised using 12-noded zero-thickness interface elements, whose behaviour was modelled independently from the surrounding soil by adopting a linear elastic-perfectly plastic Mohr-Coulomb model. For the interface shear strength, the same angle of shear resistance defined according to the analytical solution in Equation 1 was adopted. To allow for gap opening and avoid residual shear stresses on the active side of the soil-pile interface, a zero-intercept cohesion was considered along with the tension cut-off option. The elastic behaviour of the interface elements was represented with normal (K_N) and shear (K_S) interface stiffness values of 200MN/m^3 in line with the average small strain Young's modulus in the top 10m depth.

Displacement-based finite element analyses were run by applying an incremental displacement in the positive X-direction at the pile head. Given the low permeability of the Cowden clay till, all analyses were performed as undrained ("Undrained (A)" analysis option, for which a much higher value of the bulk modulus of the pore fluid (K_W) is imposed compared to the bulk modulus of the soil skeleton (K_S), as detailed in Plaxis Reference manual - Plaxis, 2021).

The load–displacement response curves at the ground level from the FE analyses are shown in Figure 8. The resulting curves using the HSS model are compared to the response curves obtained either via numerical analysis (3D FE PISA) or real scale field data (Zdravković´ et al., 2020b).

The results show a good match between the FE simulation and the field data. The loading capacity up to a maximum lateral displacement of 0.1D is predicted with a very good accuracy for both cases.

The results seem to confirm that the predictive capability of the numerical model is not affected by changes in the pile slenderness ratio or diameter.

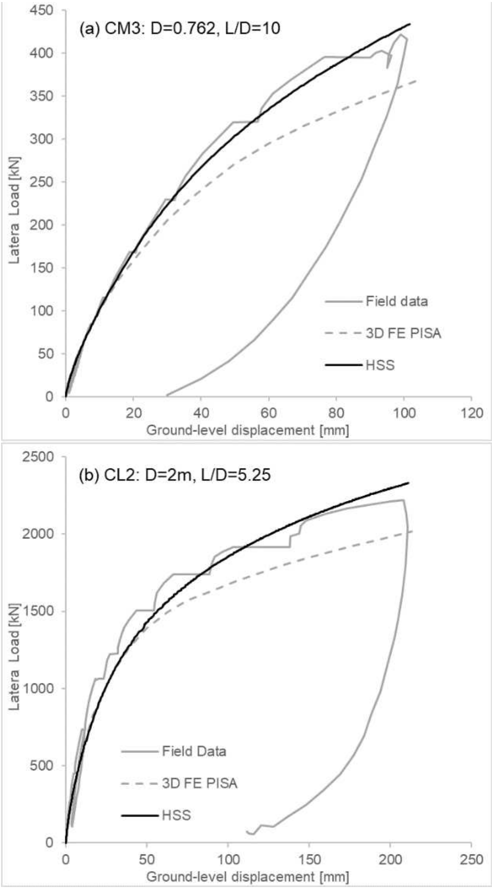

Figure 8 – Load-Displacement response

5 CONCLUSIONS

The FE analyses undertaken for the PISA project were carried out using an advanced soil model developed in the framework of critical state soil mechanics. Use of this advanced and non-commercially available model is limited to non-commercial FE packages, such as the one used in the PISA project. A few attempts have been made to replicate the PISA results using constitutive models available in commercial FE packages but none disclosed a satisfactory agreement with the pile test results.

The present paper illustrates the use of a commercially available soil constitutive model. The models adopted is the Hardening Soil model with Small strain stiffness (HSS) implemented in the FE package Plaxis 3D.

Using the soil data from the Cowden site where the full-scale pile tests were set up to carry on the PISA project, the soil parameter selection and model calibration is described, specifically based on the:

- Soil data profiles: undrained shear strength stress history and in-situ small strain stiffness.
- Strength test laboratory data such as compression triaxial tests.
- Laboratory test data exhibiting the decrease of soil modulus with strain, for instance resonant column tests.

To allow a proper formation of gapping on the active side of the monopile, a separate linear elastic – perfectly plastic model has been adopted for the simulation of the soil-steel interface.

The results presented in this paper demonstrate that a soil model available in commercial software packages, such as for example the HSS model formulated in terms of effective stresses, is suited for the calibration of the monopile-soil response springs as requested by a PISA-based design method.

AUTHOR CONTRIBUTION STATEMENT

Germano V.: Conceptualization, Methodology, Formal analysis, Writing – original draft, Writing – review & editing, Visualization, Validation. **Jaeck C.**: Methodology, Validation, Writing – review & editing.

REFERENCES

Amorosi A., Boldini, D., di Lernia, A. (2016). Seismic ground response at Lotung: Hysteretic elasto-plastic-based 3D analyses. Soil Dynamics and Earthquake Engineering, 85 (44-61).

Benz, T. (2007). Small-strain Stiffness of Soils and its Numerical Consequences. PhD Thesis, Universität Stuttgart, Germany.

Byrne, B. W., McAdam, R. A., Burd, H. J., Beuckelaers, W. J. A. P., Gavin, K. G., Houlsby, G. T., Igoe, D. J. P., Jardine, R. J., Martin, C. M., Muir Wood, A., Potts, D. M., Skov Gretlund, J., Taborda, D. M. G. & Zdravković´, L. (2020). Monotonic laterally loaded pile testing in a stiff glacial clay till at Cowden. *Géotechnique*, 70(11): 970-985. https://doi.org/10.1680/jgeot.18.PISA.003

Darendeli, M. B. and Stokoe, K. H., (2001). Development of a new family of normalised modulus reduction and material damping curves. Engrg. Rpt. GD01-1, University of Texas, Austin, Texas.

Minga, E., Burd, H. (2019). Validation of Plaxis MoDeTo based on the Cowden till PISA field tests.

Mayne, P.W., Coop, M.R., Springman, S., Zornberg, J. (2009). Geomaterial behaviour and testing. *Proceedings of 17th International Conference on Soil Mechanics and Geotechnical Engineering*. ICSMGE, Alexandria Egypt, pp. 2777-2872.

Kaltekis K., Whyte S., Vahdatirad M.J., Abyaneah, S., Burbury, D., Mclean, R., Francis, M., Hilrton, J., Berberic, S. (2023). A review of constitutive models for an FEA-based monopile design. (2023) *Proceedings of* 9th *International SUT Offshore Site Investigation and Geotechnics Conference - Innovative Geotechnologies for Energy Transition*, London, pp. 1614-1621.

PLAXIS Connect Edition V21.01. All Manuals. ©, (2021) Plaxis bv, Bentley Systems, Incorporated.

Potts, D. M. and Zdravković´, L. T., (1999). Finite element analysis in geotechnical engineering: theory. London, UK: Thomas Telford.

Roscoe, K. H. and Burland, J. B. (1968). On the generalized stress–strain behaviour of wet clay. Engineering plasticity (eds J. Heyman and F. A. Leckie), pp. 535–609. Cambridge, UK: Cambridge University Press.

Schanz, T., Vermeer, P.A., Bonnier, P.G. (1999). The hardening soil model: formulation and verification. *Proceedings of the International Symposium beyond 2000 in Computational Geotechnics*, Balkema, Amsterdam, pp. 1-16.

Surarak, C., Likitlersuang, S., Wanatowski, D., Balasubramaniam, A., Oh, E., Guan, H. (2012). Stiffness and strength parameters for hardening soil model of soft and stiff Bangkok clays. Soils and Foundations, 52(4): 682-697.

Ushev E. (2017). *Laboratory investigation of mechanical properties of Cowden till under static and cyclic conditions*. PhD Thesis, Imperial College, London. Zdravković, L., Jardine, R. J., Taborda, D. M. G., Abadias, D., Burd, H. J., Byrne, B. W., Gavin, K. G., Houlsby, G. T., Igoe, D. J. P., Liu, T., Martin, C. M., McAdam, R. A., Muir Wood, A., Potts, D. M., Skov Gretlund, J., Ushev, E. (2020a). Ground characterisation for PISA pile testing and analysis. *Géotechnique*, 70(11): 945-960. https://doi.org/10.1680/jgeot.18.PISA.001

Zdravković, L., Taborda, D. M. G., Potts D. M., Abadias D., Burd H. J., Byrne B. W., Gavin K. G., Houlsby G. T., Jardine R. J., Martin C. M., Mcadam R. A., Ushev E. (2020b). Finite-element modelling of laterally loaded piles in a stiff glacial clay till at Cowden. *Géotechnique*, 70(11): 999-1013. https://doi.org/10.1680/jgeot.18.PISA.005

APPENDIX – HSS model parameters

Layer	Top	Bottom	Secant Stiffness	Oedometric Stiffness	Unloading/Reloading Stiffness	Power stress level dependency	Cohesion	Friction Angle	Threshold Shear strain	Reference Small Strain Shear Stiffness	Earth Pressure Coefficient at rest	Overconsolidation ratio	Pre-Overburden Pressure
	from	*to*	E_{50}^{ref}	E_{oed}^{ref}	E_{ur}^{ref}	m	c'	ϕ'	$\gamma_{0.7}$	G_0^{ref}	K_0	OCR	POP
	[m]	[m]	[kPa]	[kPa]	[kPa]	[-]	[kPa]	[°]	[-]	[kPa]	[-]	[-]	[kPa]
1	0.0	-1.0	3040	2432	9121	0.5	30	35	5.70E-05	34 866	1.5	29	0.0
2	-1.0	-2.0	4180	3344	12540	0.5	60	35	7.00E-05	47 934	1.5	29	0.0
3	-2.0	-2.5	5009	4007	15027	0.5	90	35	7.70E-05	57 441	1.5	24	0.0
4	-2.5	-4.0	6460	5168	19380	0.5	70	35	8.50E-05	74 080	1.5	12	0.0
5	-4.0	-5.0	3782(*)	3026(*)	11347(*)	0.5	60	30	9.30E-05	75 515(*)	1.45	7.8	0.0
6	-5.0	-7.5	4631(*)	3705(*)	13895(*)	0.5	65	28	1.00E-04	108 550	1.0	1.0	432
7	-7.5	-10.0	6123	4898	18368	0.5	80	28	1.10E-04	139 216	1.0	1.0	460
8	-10.0	-12.5	7073	5658	21218	0.5	80	27	1.23E-04	160 816	1.0	1.0	493
9	-12.5	-15.0	8137	6509	24410	0.5	80	27	1.32E-04	185 015	1.0	1.0	513
10	-15.0	-20.0	9825	7860	29475	0.5	80	27	1.38E-04	223 397	1.0	1.0	534
11	-20.0	-25.0	11970	9576	35911	0.5	80	27	1.46E-04	272 184	1.0	1.0	560
12	-25.0	-30.0	13986	11189	41959	0.5	80	27	1.53E-04	318 018	1.0	1.0	577